Amino Acids (2014) 46:2573–2586
DOI 10.1007/s00726-014-1811-2

ORIGINAL ARTICLE

Chemical synthesis, structure–activity relationship, and properties of shepherin I: a fungicidal peptide enriched in glycine-glycine-histidine motifs

César Remuzgo · Thaís S. Oewel · Sirlei Daffre · Thiago R. S. Lopes · Fabio H. Dyszy · Shirley Schreier · Gláucia M. Machado-Santelli · M. Teresa Machini

Received: 25 March 2014 / Accepted: 9 July 2014 / Published online: 9 August 2014

Abstract Although glycine-rich antimicrobial peptides (AMPs) are found in animals and plants, very little has been reported on their chemistry, structure activity-relationship, and properties. We investigated those topics for *Shepherin I* (*Shep I*), a glycine-rich AMP with the unique amino acid sequence G^{1}YGGHGGHGGHGGHGGHGGH-GHGGGGHG^{28}. *Shep I* and analogues were synthesized by the solid-phase method at 60 °C using conventional heating. Purification followed by chemical characterization confirmed the products' identities and high purity. Amino acid analysis provided their peptide contents. All peptides were active against the clinically important *Candida* species, but ineffective against bacteria and mycelia fungi. Truncation of the *N*- or C-terminal portion reduced *Shep I* antifungal activity, the latter being more pronounced. Carboxyamidation of *Shep I* did not affect the activity against *C. albicans* or *C. tropicalis*, but increased activity against *S. cerevisiae*. Carboxyamidated analogues *Shep I (3-28)a* and *Shep I (6-28)a* were equipotent to *Shep I* and *Shep Ia* against *Candida* species. As with most cationic AMPs, all peptides had their activity significantly reduced in high-salt concentrations, a disadvantage that is defeated if 10 μM $ZnCl_2$ is present. At 100 μM, the peptides were practically not hemolytic. *Shep Ia* also killed *C. albicans* MDM8 and ATCC 90028 cells. *Fluo-Shep Ia*, an analogue labeled with 5(6)-carboxyfluorescein, was rapidly internalized by *C. albicans* MDM8 cells, a salt-sensitive process dependent on metabolic energy and temperature. Altogether, such results shed light on the chemistry, structural requirements for activity, and other properties of candidacidal glycine-rich peptides. Furthermore, they show that *Shep Ia* may have strong potential for use in topical application.

Keywords Synthesis at 60 °C · Antimicrobial peptide · Fungicidal activity · Structure–activity relationship

Abbreviations

Shep I	*Shepherin I*
SAR	Structure–activity relationship
AMPs	Antimicrobial peptides
MIC	Minimal inhibitory concentration
Fluo	5(6)-Carboxyfluorescein
GRP	Glycine-rich peptide or protein
Boc	*Tert*-butyloxycarbonyl
Fmoc	9-Fluorenylmethyloxycarbonyl
Tos	Tosyl

Electronic supplementary material The online version of this article (doi:10.1007/s00726-014-1811-2) contains supplementary material, which is available to authorized users.

C. Remuzgo · T. S. Oewel · T. R. S. Lopes · M. Teresa Machini (✉)
Laboratory of Peptide Chemistry, Department of Biochemistry, Institute of Chemistry, University of São Paulo, P.O. Box 26077, 05513-970 São Paulo, SP, Brazil
e-mail: mtmachini@iq.usp.br

Present Address:
C. Remuzgo
Special Laboratory of Pain and Signaling, Butantan Institute, São Paulo, Brazil

S. Daffre
Department of Parasitology, Institute of Biomedical Sciences, University of São Paulo, São Paulo, Brazil

F. H. Dyszy · S. Schreier
Laboratory of Structural Biology, Department of Biochemistry, Institute of Chemistry, University of São Paulo, São Paulo, Brazil

G. M. Machado-Santelli
Department of Cell and Developmental Biology, Institute of Biomedical Sciences, University of São Paulo, São Paulo, Brazil

PAM	4-Hydroxymethyl-phenylacetamidomethyl
NMP	*N*-methyl-2-pyrrolidone
DMSO	Dimethyl sulfoxide
PBS	Phosphate-buffered saline
IGP	Isotonic glucose phosphate
PBC	Phosphate-borate-citrate
TFE	2,2,2-Trifluoroethanol
SDS	Sodium dodecyl sulfate
PDB	Potato dextrose broth

Introduction

Candidemia has become a major concern in tertiary-care hospitals worldwide because it causes morbidity and mortality in hospitalized patients, especially those who are immunocompromised (Hoffmann-Santos et al. 2013). In Brazil, this is a huge problem, as the incidence of this type of invasive infection is 2–10 times higher than that documented in the USA and Europe (Colombo et al. 2009; Hoffmann-Santos et al. 2013). Unfortunately, the treatment of candidemia has been hampered by the limited anticandidal—rather than candidacidal—activity of the current antibiotics, as well as by resistance of *Candida* species to them. Hence, the knowledge on compounds capable of killing such cells has been considered critical for the development of a new generation of candidacidal drugs (Matejuk et al. 2010).

So far, the only antifungal lipopeptides approved by the US Food and Drug Administration (FDA) against candidemia and invasive aspergillosis are caspofungin, anidulafungin, and micafungin—three members of the echinocandin family of β-glucan inhibitors (Matejuk et al. 2010; Eschenauer et al. 2014). In fact, there are two groups of antifungal peptides: (1) those with primarily antifungal properties, which include 1,3-β-glucan synthesis inhibitors (echinocandins, pneumocandins), cell wall chitin inhibitors (nikkomycins, polyoxins, aurebasidins), and membrane-active, selective antimicrobial peptides (Rs-AFP2, heliomicin, drosomycin), and (2) those with broad-spectrum antimicrobial activity, such as cecropins, magainins, protegrins, and dermaseptins (Matejuk et al. 2010).

In this context, antimicrobial peptides (AMPs) have been extensively studied. The main reasons for such increasing interest are the following: (1) since AMPs work through mechanisms different from those of non-peptide antibiotics, they can serve as templates in the design of AMP mimetics; (2) the mode of action of AMPs involves cell membrane damage, so AMPs can enhance our understanding of membrane permeabilization through pore formation and membrane fusion; (3) AMPs can serve as antibiotic drugs for topical uses; (4) certain AMPs are cell-penetrating peptides, and thus, they are capable of delivering drugs inside the cell (Matejuk et al. 2010; Bechinger 2013). Therefore, in the last two decades, antifungal peptides have become potential candidates for the development of more potent, specific, and non-toxic antimycotic drugs.

Peptides containing 15–70 % glycine (so-called glycine-rich peptides) have been found in plants and their expression is associated with physical (cold, light, wound), chemical (hormones), and biological (pathogens, development, circadian rhythms) factors, revealing their key roles in cellular processes (Sachetto-Martins 2000; Ringli et al. 2001). Glycine-rich AMPs have also been found in insects, isopods, spiders, crabs, frogs, and plants, commonly in the *Brassicaceae*, *Solanaceae*, and *Panicoideae* families (Bulet et al. 1999; Park et al. 2000; Lorenzini et al. 2003; De Souza Cândido et al. 2011). The majority of them have been reported to inhibit the growth of fungi and/or Gram-negative bacteria (Lorenzini et al. 2003), such as gloverin, ctenidins, Pg-AMP, and leptoglycin (active against Gram-negative bacteria) (Bulet et al. 1999; Baumann et al. 2010; Pelegrini et al. 2008; Sousa et al. 2009), as well as AFP, holotricin-3, tenecin-3, and glycine/histidine-rich peptides that are active against fungi (Iijima et al. 1993; Lee et al. 1995; Kim et al. 2001). The minority, which are active against Gram-positive bacteria, include armadillidin and hyastatin (Herbinière et al. 2005; Sperstad et al. 2009). Interestingly, little is known about their functions and secondary structures, a fact that may be related to difficulties found during the syntheses of glycine-rich peptides (Remuzgo et al. 2009).

Histidine-rich peptides, such as the histatins and LAH4, can act not only as antimicrobial agents, but also as DNA delivery vehicles (Bechinger 2013; Nakagawa et al. 2013). This dual functionality indicates that these AMPs can operate with at least two distinct modes of bacterial killing and gives them the potential to be used in a variety of infection diseases. A high percentage of patients with cystic fibrosis have lung infection caused by *Pseudomonas aeruginosa* and, for instance, it has been shown that LAH4 is highly active against this pathogenic bacteria at an acidic pH (Bechinger 2013).

Shepherin I (*Shep I*) is a 28-mer AMP isolated from the root of the plant *Capsella bursa-pastoris* (family Brassicaceae), known by its common name *shepherd's purse*, and characterized by its almost exclusive glycine (67.9 %) and histidine (28.6 %) contents, along with the presence of six tandem repeats of the motif Gly-Gly-His (GGH). This glycine- and histidine-rich peptide was reported to be active against Gram-negative bacteria and yeast phase-fungi, as well as to show moderate activity against mycelial fungi (Park et al. 2000).

In view of the above considerations, as well as its atypical amino acid sequence (composed almost exclusively of Gly and His, only one Tyr, and six repetitive motifs of

Gly-Gly-His, a copper- and nickel-chelating tripeptide) and, especially, the lack of knowledge of the synthesis and properties of glycine- and histidine-rich peptides, we synthesized *Shep I* and its truncated, amidated, and fluorescently labeled analogues by the solid-phase method at 60 °C. We then purified and chemically characterized them, tested them against bacteria and fungi—including *Candida* strains and *Saccharomyces cerevisiae*—at low- or high-salt concentration in the absence or presence of Zn^{2+} ions, and evaluated their toxicity to human erythrocytes. Also, we determined the killing kinetics of *Shep Ia* against two different strains of *C. albicans* and performed experiments to determine the initial steps toward disclosing its mode of action.

Materials and methods

Reagents

N-α-Fmoc-amino acids, N-α-Boc-amino acids, and Boc-His(Tos)-PAM resin (0.69 mmol/g, 100–200 mesh) were obtained from Bachem California (Torrance, CA, USA) and Novabiochem AG (Laüfelfingen, Switzerland). Cross-linked Ethoxylate Acrylate Resin (CLEAR®) amide resin (0.35 mmol/g, 100–200 mesh) and Fmoc-Gly-CLEAR resin (0.48 mmol/g, 100–200 mesh) were obtained from Peptide International, Inc. (Louisville, KY, USA). 5(6)-Carboxyfluorescein (*Fluo*), *N*-hydroxybenzotriazole (HOBt), *N,N′*-diisopropylcarbodiimide (DIC), and benzotriazole-1-yl-oxy-tris-(dimethylamino)-phosphonium hexafluorophosphate (BOP) were purchased from Sigma Chemical Co. (St. Louis, MO, USA) and Novabiochem AG (Laüfelfingen, Switzerland). Analytical- or chromatographic-grade solvents and other reagents were obtained from Merck KgaA (Darmstadt, Germany), Sigma Chemical Co. (St, Louis, MO, USA), LabSynth (São Paulo, SP, Brazil), or Vetec (Rio de Janeiro, RJ, Brazil).

Comparative amino acid sequence analysis

A PSI-BLAST (Altschul et al. 1997) search against the non-redundant protein sequence database at NCBI was performed to elucidate the relationship between the deduced amino acid sequence of the *shep-grp* gene (Genbank accession number AAG09424; named Shep-GRP, which encodes *shepherin I* and *shepherin II*) with other homologous sequences at the primary amino acid sequence level. A multiple alignment of *Shep-GRP* with the highest score sequences obtained in the PSI-BLAST search was performed using the MUSCLE program (Edgar 2004).

Peptide synthesis, purification, and chemical characterization

All syntheses were performed manually by the stepwise solid-phase method at 60 °C using conventional heating, customized protocols, CLEAR amide or Fmoc-Gly-CLEAR (cited above) as resins, DIC/HOBt (1:1) as coupling reagents, and 20 % DMSO/NMP as the solvent system (Varanda and Miranda 1997; Souza et al. 2004; Remuzgo et al. 2009; Loffredo et al. 2009). The carboxyl-free peptides *Shep I* and *Shep I (3-28)* and the carboxyamidated analogues were assembled on Fmoc-Gly-CLEAR acid and CLEAR amide resins, respectively, by Fmoc chemistry. *Shep I (1-20)*, *Shep I (3-20)*, *Shep I (6-20)*, *Shep I (12-20)*, *Shep I (15-20)*, and *Shep I (18-20)* were built up on Boc-His(Tos)-PAM resin by the Boc strategy (Table 1). The coupling of the 5(6)-carboxyfluorescein (*Fluo*) to fully protected *Shep Ia*-CLEAR amide was performed with 5

Table 1 Nomenclature, sequence, and chemical characterization data of the peptides synthesized and studied

Peptide	Sequence	Net charge (*Q*)	Purity[a] (%)	LC/ESI–MS calculated/measured
Shep I	GYGGHGGHGGHGGHGGHGGHGHGGGGHG	8	96	2 362.3/2 362. 3 $[M+H]^+$
Shep I (3-28)	GGHGGHGGHGGHGGHGGHGHGGGGHG	8	97	2 142.1/2 142.4 $[M+H]^+$
Shep I (1-20)	GYGGHGGHGGHGGHGGHGGH	6	97	1 745.7/1 746.0 $[M+H]^+$
Shep I (3-20)	GGHGGHGGHGGHGGHGGH	6	97	1 525.5/1 526.6 $[M+H]^+$
Shep I (6-20)	GGHGGHGGHGGHGGH	5	99	1 274.2/1 274.4 $[M+H]^+$
Shep I (9-20)	GGHGGHGGHGGH	4	95	1 023.0/1 023.2 $[M+H]^+$
Shep I (12-20)	GGHGGHGGH	3	97	771.8/772.4 $[M+H]^+$
Shep I (15-20)	GGHGGH	2	99	520.5/521.2 $[M+H]^+$
Shep I (18-20)	GGH	1	99	269.3/270.1 $[M+H]^+$
Shep Ia	GYGGHGGHGGHGGHGGHGGHGHGGGGHG-NH_2	9	97	2 361.3/2 361.0 $[M+H]^+$
Shep I (3-28)a	GGHGGHGGHGGHGGHGGHGHGGGGHG-NH_2	9	95	2 141.1/2 141.6 $[M+H]^+$
Shep I (6-28)a	GGHGGHGGHGGHGGHGHGGGGHG-NH_2	8	95	1 889.9/1 890.8 $[M+H]^+$

[a] Purity was estimated by reversed-phase high-performance liquid chromatography (RP-HPLC)

equiv. of *Fluo*, 5 equiv. of BOP and 5 equiv. of HOBt in 20 % DMSO/NMP for 2 h at room temperature.

The peptide resins obtained were submitted to cleavage of the peptide from the resin and simultaneous full deprotection in the presence of: (1) hydrogen fluoride and anisole (1 %) for 90 min at 0 °C (Boc strategy), and (2) 95 % TFA/2.5 % triisopropylsilane/2.5 % water for 4 h at 37 °C (Fmoc strategy). The crude peptides were precipitated from the reaction mixtures with ice-cold diisopropyl ether, separated by centrifugation, extracted with 0.1 % TFA/water and 50 % acetonitrile/0.09 % TFA/water, lyophilized, and then weighed.

The crude synthetic peptides were loaded on a Waters RP-HPLC system, model 600E [quaternary Waters Delta 600 pump, Waters 600 gradient controller, Waters 2487 Dual Absorbance Detector (Milford, MA)], equipped with a 3725i-119 Rheodyne injector, Vydac C18 preparative column (10 µm, 300 Å, 2.2 × 25 cm), and Kipp and Zonen SE124 recorder. Fractions were analyzed by RP-HPLC using a Waters system (two 510 pumps, a 680 automated gradient controller, and a 486 tunable UV–VIS absorbance detector) equipped with a 7125 Rheodyne injector, analytical C18 column (5 µm, 300 Å, 0.46 × 25 cm), and 745B Waters integrator. Those containing the purified peptides were pooled and lyophilized. The purified peptides were characterized by liquid chromatography/electrospray ionization–mass spectrometry (LC/ESI–MS) using a Micromass Quatro II triple quadrupole (ESI) mass spectrometer (Altrincham, UK) online coupled to a Shimadzu RP-HPLC VP Series column (Kyoto, Japan), and by amino acid analysis using a Beckman automated amino acid analyzer, model 7300 (Palo Alto, CA).

Microorganisms

Gram-positive bacteria included *Micrococcus luteus* A270, *Staphylococcus aureus* ATCC 6538, and *Enterococcus faecalis* ATCC 19433. Gram-negative bacteria included *Pseudomonas aeruginosa* ATCC 14502, *Escherichia coli* SBS 363 (P. Bulet, CNRS, Strasbourg, France), *Enterobacter cloacae* K12 (H. G. Boman, Stockholm University, Sweden), and *Serratia marcescens* CDC 4124. The yeasts were *Candida albicans* MDM8 (Department of Microbiology, Institute of Biomedical Science, University of São Paulo, Brazil), *Candida albicans* ATCC 90028 and fluconazole-resistant *Candida albicans* HU168 (N. Lincopan, Institute of Biomedical Science, University of São Paulo), *Candida parapsilosis* ATCC 22019 and *Candida krusei* ATCC 6258 (S. R. Almeida, Faculty of Pharmaceutical Sciences, University of São Paulo), *Candida tropicalis* Squibb 1600 (H. Koenig, Laboratory of Mycology, University of Strasbourg, France), and *Saccharomyces cerevisiae* ATCC 2601. The Mycelial fungi included *Aspergillus flavus* NCPF 2199 and *Aspergillus fumigatus* NCPF 2109 (E. B. Bergter, Microbiology Institute, Rio de Janeiro Federal University, Brazil).

Antibacterial activity

Antibacterial activity was evaluated by liquid growth inhibition assay as previously described (Ehret-Sabatier et al. 1996). Briefly, each well of the sterile, 96-well microplates contained 10 µL of twofold serial dilutions of purified peptides with water Milli Q grade, 18.2 MΩ (final concentration: 0.195–100 µM), and 90 µL of bacterial suspension (starting optical density, $OD_{595nm} = 0.001$) in peptone water broth (with salt or no salt, pH 7.4). Microbial growth was quantified by monitoring the OD of the microplates at 595 nm after incubation for 18 h at 30 °C. The minimal inhibitory concentration (MIC) was defined as the lowest concentration that inhibited the visible microbial growth. At least three independent experiments were performed.

Antifungal activity

The antifungal activity was evaluated using a liquid growth inhibition assay as previously described (Fehlbaum et al. 1994). Briefly, each well of the sterile, 96-well microplates contained 10 µL of twofold serial dilutions of each purified peptide (final concentration: 0.195–100 µM), 10 µL of water, and 80 µL of fungal suspension (starting $OD_{595nm} = 0.001$) in 1/2 potato dextrose broth (PDB). Microbial growth was measured and the MICs were determined as described above. At least three independent experiments were performed.

To evaluate the effect of NaCl and $ZnCl_2$ on antifungal activity against *C. albicans* MDM8, 10 µL of concentrated NaCl or $ZnCl_2$ solution instead of 10 µL of water were added to the cell suspension to give a final concentration of 4.3–137.0 mM NaCl or 5–100 µM $ZnCl_2$. As controls, *C. albicans* MDM8 cells were grown in the absence and presence of 137.0 mM NaCl or 100 µM $ZnCl_2$.

Hemolytic activity

Hemolytic activity was measured as previously described (Helmerhorst et al. 1999b; Machado et al. 2007). Briefly, fresh human blood was obtained from three healthy individuals and collected in BD Vacutainer® spray-coated K2EDTA tubes (BD, Oakville, ON, Canada). The erythrocytes were harvested from blood by centrifugation at 4 °C and 300 g for 5 min, and washed three times in phosphate-buffered saline (PBS, 10 mM Na_2PO_4 containing 140 mM NaCl and 2.7 mM KCl, pH 7.4 and 313 mOsm/kg of water). Next, the erythrocytes suspended in PBS were diluted to 1.11 % in PBS or isotonic glucose phosphate

(IGP) buffer (1 mM K_2PO_4, pH 7.4, supplemented with 287 mM glucose, 314 mOsm/kg of water).

Twofold serial dilutions of the peptides (20 μL; final concentration: 0.195–100 μM) were incubated in Eppendorf tubes containing 180 μL of erythrocyte suspension (final concentration: 1 %). After incubation for 1 h at 37 °C, the tubes were centrifuged for 5 min at 300 g and 4 °C, and 100 μL of supernatant were transferred to 96-well plates. Hemolysis was then monitored at 405 nm. PBS or IGP buffer was used as a negative control and 1 % sodium dodecyl sulfate (SDS) in PBS or IGP buffer was used as a positive control. The percentages of hemolysis were calculated by: $[(A_{405nm}$ sample $- A_{405nm}$ negative control)/$(A_{405nm}$ positive control $- A_{405nm}$ negative control)$] \times 100$. At least three independent experiments were performed.

Killing kinetics of *Shep Ia* against *C. albicans*

A suspension of *C. albicans* MDM8 cells in exponential growth (2.5×10^4 CFU/mL) were incubated with 62.5 μM *Shep Ia* (5 MIC) for different time intervals (0, 10, 20, 30, 60, 120, and 240 min). Samples were then removed, serially diluted with PDB, and plated in Sabouraud agar. After incubation of the plates at 30 °C for 24 h, colony forming units (CFU) were counted. Three independent experiments were performed. Similar experiments were performed using *C. albicans* ATCC 90028 and *Shep Ia* at MIC and 2 MIC.

Membrane permeability assay

A suspension of *C. albicans* MDM8 cells in exponential growth (2×10^6 CFU/mL) was incubated with 12.5 μM *Shep Ia* (MIC) for 60 min at 37 °C. Subsequently, the cells were treated with the Live/Dead BacLigth viability kit (mixture of SYTO® 9 and propidium iodide dyes, Molecular Probes®, Life Technologies, USA) following the manufacturer's instructions. Identical profiles were verified in three independent experiments. The samples were mounted on polylysine-coated glass slides and analyzed using a Zeiss fluorescence microscopy Axiovert S100 (Carl Zeiss MicroImaging GmbH, Göttingen, Germany).

The assay employs SYTO® 9 (green fluorescence) dye, which is permeable to the intact membranes of viable cells, and propidium iodide (red fluorescence) dye, which is permeable to the damaged membranes of unviable cells. Water and isopropanol are used as negative and positive controls, respectively.

Confocal laser scanning microscopy

Candida cells were grown overnight at 37 °C in 3 mL of Sabouraud dextrose broth in a shaking incubator. The cells were diluted (1:100) in Sabouraud dextrose broth and incubated for 4 h at 30 °C to enrich the population of exponentially growing cells, and then the cells were adjusted to 2×10^6 CFU/mL. The cell suspension (200 μL, 2×10^6 CFU/mL) was incubated with 3.13 μM *Fluo-Shep Ia* (1x MIC) for 15 min at 30 °C, centrifuged for 5 min at 10,000*g* and 5 °C, and washed three times with PDB. Intracellular localization of *Fluo-Shep Ia* in *Candida* cells were analyzed in a Carl Zeiss LSM 510 laser scanning confocal microscope (Carl Zeiss MicroImaging GmbH, Göttingen, Germany) equipped with an argon/krypton laser. At least three independent experiments were performed.

FACS analysis

C. albicans MDM8 cells were grown overnight at 37 °C in 3 mL of Sabouraud dextrose broth (a solution with nutrients) in a shaking incubator. The resulting suspension was diluted in Sabouraud dextrose broth (1:100; v/v) and incubated for another 4 h at 30 °C to enrich the cell population exponentially (to guarantee that the cells are at the log phase of growth). The suspension was centrifuged at 10,000*g* and 5 °C for 5 min, washed three times with PDB (potato dextrose broth), and adjusted to 2×10^6 CFU/mL. The fluorescently labeled peptide *Fluo-Shep Ia* was added to 1 mL of cell suspension at 3.13 μM, a peptide concentration previously determined to inhibit *C. albicans* MDM8 cell growth. The new cell suspension (*Fluo-Shep Ia* + *C. albicans* MDM8 cells) was incubated for 15 min at 0 °C or 30 °C (to determine the effect of temperature on peptide penetration into the cells), in the absence or presence of 0.05 % NaN_3 [to determine whether peptide penetration into the cells occurs with adenosine triphosphate (ATP) depletion; NaN_3 is known to inhibit the last stage of cell respiration with ATP synthesis], or in various concentrations of NaCl (4.28–34.25 mM; to determine the effect of salt concentration on peptide penetration into the cells). Next, the cells were centrifuged for 5 min at 10,000*g* and 5 °C, washed three times with PDB, and suspended in 1 mL of PBS for the detection and quantification of fluorescence. Indeed, cell fluorescence is expected to increase if *Fluo-Shep Ia* penetrates the cell. The quantification of cells with no uptake of *Fluo-Shep Ia* was performed by calculating the percentages of events (cells) in the M1 marker. The M1 marker indicates negative events and the M2 marker indicates positive events. Internalization of *Fluo-Shep Ia* was determined using a Cytomics FC500 flow cytometry system (Beckman Coulter Inc., CA, USA).

Circular dichroism (CD) spectroscopy

Circular dichroism (CD) spectra were acquired on a Jasco J-710 spectropolarimeter using a quartz cell with 0.5-mm

path length. A peptide concentration of 100 μM and three different environments were used: 10 mM phosphate-borate-citrate (PBC) buffer, pH 5.0, and 60 % trifluoroethanol (TFE), or 20 mM SDS in 10 mM PBC, pH 5.0. All spectra were derived from eight scans per sample recorded at 22 °C, measured between 190 and 260 nm, and obtained by subtracting the spectra of the buffer with or without TFE and SDS, respectively.

Results

Sequence analysis of the deduced amino acid sequences of the *shep-grp* gene

The deduced amino acid sequences of the s*hep-grp* gene (Genbank accession number AAG09424), named *Shep-GRP*, encodes a single polypeptide composed by: (1) a *N*-terminal putative signal peptide sequence, (2) the antimicrobial shepherins sequences *Shep I* (GYGGHG GHGGHGGHGGHGGHGGGGHG) and *Shep II* (GYHGGHGGHGGGYNGGGGHGGHGGGYNGGGHH GGGGHG) separated by a dipeptide, and (3) a C-terminal peptide (Park et al. 2000). The comparison of the *Shep-GRP* sequence with sequences available in the non-redundant database at NCBI using PSI-BLAST showed that, according to the *N*-terminal putative signal peptide sequence, this peptide belongs to the GRP superfamily (pfam07172). This family contains GRPs, induced in response to various stresses, as well as nodulins 16 and 24, found in the peribacteroid membrane of root nodules that is an essential feature in symbioses with nitrogen-fixing bacteria (Finn et al. 2008).

Shep-GRP shares 79 and 81 % identity with a hypothetical GRP from *Arabidopsis lyrata* and with *AtGRP9* from *Arabidopsis thaliana*, respectively (Fig. 1).

Peptide design, synthesis and antimicrobial activity

To elucidate the minimal structure required for the antimicrobial activity of *Shep I*, we synthesized it and a series of carboxyl-free and carboxyamidated analogues, including truncated ones (Table 1). These compounds would allow us to examine the importance of the GGH repeats, of the *N*-terminal dipeptide G^1Y^2, and of the C-terminal octapeptide ($G^{21}HGGGGHG^{28}$) on the antimicrobial activity. The overall purities were higher than 95 % and the molar masses were in perfect agreement with those expected (Supplemental material, Fig. S1). Peptide contents of the purified peptides were considered for the bioassays.

Shep I was inactive against Gram-positive bacteria (*Staphylococcus aureus ATCC 6538*, *Micrococcus luteus A270*, *Enterococcus faecalis ATCC 19433*) and active against fungi (*C. albicans* MDM8, *C. albicans* ATCC 90028, *C. albicans* HU 168 [fluconazole resistant], *C. parapsilosis* ATCC 22019, *C. krusei* ATCC 6258, *C. tropicalis* Squibb 1600 and *S. cerevisiae* ATCC 2601), corroborating the work of Park et al. (2000). It was inactive against Gram-negative bacteria (*E. coli* SBS 363, *Pseudomonas aeruginosa* ATCC 14502, *Enterobacter cloacae* K12, S*erratia marcescens* CDC 4124) and filamentous fungi (*Aspergillus flavus* NCPF 2199 and *Aspergillus fumigatus* NCPF 2109) up to 100 μM. Peptide Hb40-61a (an amidated fragment 40-61 of bovine α-hemoglobin; Sforça et al., 2005) was also tested against some of these bacteria strains and showed to be active.

The results obtained with the *Candida* strains used are listed in Table 2, which also shows the results obtained with melittin (a well-known antimicrobial peptide) and amphotericin B (a commercial non-peptide antifungal drug), both used as controls in the tests against *C. albicans* ATCC 90028. As can be seen in the table, the decrease in *Shep I* antifungal activity caused by the deletion of the two amino acids at the *N*-terminal end was more evident for

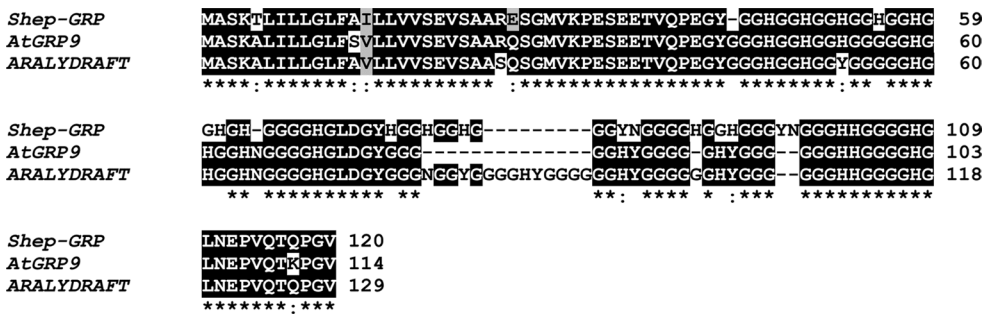

Fig. 1 Amino acid sequence alignment of *Shep-GRP* with other GRP proteins. The deduced amino acid sequence of the *shep-grp* gene, named *Shep-GRP* and containing *Shep I* and *Shep II*, was aligned with *GRP9* from *Arabidopsis thaliana* (*AtGRP9*, NCBI reference sequence NP_001031332.1) and a hypothetical GRP from *Arabidopsis lyrata lyrata* (*ARALYDRAFT*, NCBI reference sequence XP_002883695) using the MUSCLE program (http://www.ebi.ac.uk/Tools/msa/muscle/). Identical amino acid residues are indicated as *black boxes*, whereas similar amino acids are indicated as *gray boxes*

Table 2 Anticandidal activity of *Shep I* and its synthetic analogues in low-ionic-strength PDB medium

Peptide	MIC (μM)						
	C. albicans MDM8	*C. albicans* ATCC 90028	*C. albicans* HU 168	*C. parapsilosis* ATCC 22019	*C. krusei* ATCC 6258	*C. tropicalis* Squibb 1600	*S. cerevisiae ATCC 2601*
Shep I	12.5	25.0	25.0	6.25	50.0	1.56	12.5
Shep I (3-28)	25.0	>100.0[a]	100.0	6.25	>100.0	3.13	25.0
Shep I (1-20)	50.0	>100.0	>100.0	12.5	>100.0	3.13	50.0
Shep I (3-20)	100.0	>100.0	>100.0	12.5	>100.0	6.25	50.0
Shep I (6-20)	>100.0	>100.0	>100.0	25.0	>100.0	25.0	>100.0
Shep I (9-20)	>100.0	>100.0	>100.0	100.0	>100.0	100.0	>100.0
Shep I (12-20)	>100.0	>100.0	>100.0	>100.0	>100.0	>100.0	>100.0
Shep I (15-20)	>100.0	>100.0	>100.0	>100.0	>100.0	>100.0	>100.0
Shep I (18-20)	>100.0	>100.0	>100.0	>100.0	>100.0	>100.0	>100.0
Shep Ia	12.5	12.5	25.0	6.25	25.0	1.56	6.25
Shep I (3-28)a	12.5	25.0	25.0	6.25	50.0	1.56	6.25
Shep I (6-28)a	12.5	>100.0[a]	50.0	6.25	100.0	1.56	12.5

The anticandidal activity was measured by liquid growth inhibition assay. The minimal inhibitory concentration (*MIC*) was defined as the lowest concentration that inhibited the visible microbial growth

[a] Partial inhibition. *MIC*s for melittin and amphotericin B against *C. albicans ATCC 90028* were 25.0 and 1.1–2.2 *μM*, respectively

C. albicans ATCC 90028 and *C. albicans* HU 168 (fourfold), and for *C. krusei* ATCC 6258 than for *C. albicans* MDM8, *C. tropicalis* Squibb 1600, and *S. cerevisiae* ATCC 2601 (twofold). A similar effect was observed for C-terminal-end truncation of *Shep I*.

Regarding the analogues related to the central portion of the molecule, those encompassing four and five of the six repeats of *Shep I*'s GGH motifs (*Shep I* [*6-20*] and *Shep I* [*9-20*]) inhibited the growth of *C. parapsilosis* ATCC 22019 and *C. tropicalis* Squibb 1600. However, these peptides and those containing one to three of such motifs (*Shep I* [*18-20*]–*Shep I* [*12-20*]) were completely inactive against *C. albicans* MDM8, *C. albicans* ATCC 90028, *C. albicans* HU168, *C. parapsilosis* ATCC 22019, *C. krusei* ATCC 6258, *C. tropicalis* Squibb 1600, and *S. cerevisiae* ATCC 2601 (MIC >100 μM). On the other hand, the analogue containing six GGH-motif repeats (*Shep I* [*3-20*]) was active against *C. albicans* MDM8, *C. parapsilosis* ATCC 22019, *C. tropicalis* Squibb 1600, and *S. cerevisiae* ATCC 2601.

Although the carboxyamidation of *Shep I* (to give *Shep Ia*) did not significantly affect its antifungal activity, carboxyamidation of the truncated analogues *Shep I (3-28)* and *Shep I (6-28)*—to give *Shep I (3-28)a* and *Shep I (6-28a*—significantly enhanced their activities. In fact, these two amidated truncated analogues were as active as *Shep I* and *Shep Ia*, so they are able to mimic *Shep I*.

Effect of ionic strength on antifungal activity

The assays performed with the carboxyamidated analogues *Shep Ia*, *Shep I (3-28)a*, and *Shep I (6-28)a*, and with the carboxyl-free analogues *Shep I (3-28), Shep I (1-20)*, and *Shep I (3-20)* against *C. albicans* MDM8 in the absence or presence of NaCl (4.3–137.0 mM) revealed the following results. At 4.3 mM NaCl, the antifungal activity of the carboxyl-free analogues was fully inhibited, and that of *Shep I (3-28)a* or *Shep I (6-28)a* was reduced (two or fourfold, respectively). At 17.1 mM NaCl, *Shep Ia* and *Shep I (3-28)a* were four and eightfold less active, respectively, and *Shep I (6-28)a* was inactive. At 34.3 mM NaCl or at higher salt concentrations, no analogue tested was active (Table 3).

Effect of $ZnCl_2$ concentration on antifungal activity

Evaluation of the antifungal activity of *Shep Ia* against *C. albicans* MDM8 in the absence and presence of various concentrations of $ZnCl_2$ (5–100 μM) showed that antifungal activity increases fourfold in 5 μM $ZnCl_2$ and eightfold at concentrations ≥10 μM $ZnCl_2$. Therefore, we used 10 μM in the next experiments with *Shep I*, the carboxyamidated analogues, *C. albicans* MDM8, *C. albicans* ATCC 90028, and *C. albicans* HU168.

As shown in Table 4, the presence of Zn^{2+} greatly enhanced the activity of *Shep Ia* against *C. albicans* MDM8, *C. albicans* HU168 (eightfold), and *C. albicans* ATCC 90028 (twofold), as well as that of *Shep I*, *Shep I (3-28)a*, and *Shep I (6-28)a* against *C. albicans* MDM8 and *C. albicans* HU168 (fourfold).

Hemolytic activity

When *Shep Ia* and its truncated analogues *Shep I (3-28) a* and *Shep I (6-28)a* were tested for their toxicity against

Table 3 Influence of salt concentration on activity of *Shep I* and analogues against *C. albicans* MDM8

The anticandidal activity assays employed different final concentrations (4.3–137 *mM*) of *NaCl*. As a control, *C. albicans* MDM8 cells were grown in the absence and presence of 137 *mM NaCl*

Peptide	NaCl in PDB medium						
	No salt	4.3 mM	8.6 mM	17.1 mM	34.3 mM	68.5 mM	137.0 mM
	MIC (μM)						
Shep Ia	12.5	12.5	25.0	50.0	>100.0	>100.0	>100.0
Shep I (3-28)a	12.5	25.0	50.0	100.0	>100.0	>100.0	>100.0
Shep I (6-28)a	12.5	50.0	100.0	>100.0	>100.0	>100.0	>100.0
Shep I (3-28)	25.0	>100.0	>100.0	>100.0	>100.0	>100.0	>100.0
Shep I (1-20)	50.0	>100.0	>100.0	>100.0	>100.0	>100.0	>100.0
Shep I (3-20)	100.0	>100.0	>100.0	>100.0	>100.0	>100.0	>100.0

Table 4 Antifungal activity of *Shep Ia* against *Candida* strains in the absence and presence of 10 μM $ZnCl_2$

The anticandidal activity was measured at 10 *μM* $ZnCl_2$. As a control, *C. albicans MDM8* cells were grown in the absence and presence of 10 *μM* $ZnCl_2$

[a] Partial inhibition

Peptide	MIC (μM)					
	C. albicans MDM8		*C. albicans* ATCC 90028		*C. albicans* HU 168	
	No Zn^{2+}	Zn^{2+}	No Zn^{2+}	Zn^{2+}	No Zn^{2+}	Zn^{2+}
Shep I	12.5	3.13	25	N.D.	25.0	6.25
Shep Ia	12.5	1.56	12.5	6.25	25.0	3.13
Shep I (3-28)a	12.5	3.13	25.0	25.0	25.0	6.25
Shep I (6-28)a	12.5	3.13	>100.0[a]	>100.0[a]	50.0	12.5

human erythrocytes in PBS (high ionic strength) and in IGP buffer (low ionic strength), the carboxyamidated analogues caused no hemolysis in PBS buffer. In IGP buffer, *Shep I (3-28)a* and *Shep I (6-28)a* were not hemolytic, but *Shep Ia* produced 18 % hemolysis at 100 μM (concentration equivalent to 8 MIC against *C. albicans* MDM8). For details, see Fig. S2 in Supplemental Material.

Killing kinetics of *Shep Ia* in *C. albicans*

When *Shep Ia* was incubated for different time intervals with *C. albicans* MDM8 at 5 MIC (62.5 μM), it killed 98 % of the cells in 10 min. No CFUs were detected in 30 min of incubation (see Fig S3 in Supplemental Material). When the same experiment was done with *Shep Ia* at its MIC or 2 × MIC using *C. albicans* ATCC 90028, the peptide was able to inhibit cell growth at 12.5 μM (MIC) and kill all cells in 4 h at 25.0 μM (2 MIC).

Live/dead cell viability assay

C. albicans MDM8 cells treated with 12.5 μM *Shep Ia* (1x MIC) for 1 h did not present considerable red fluorescence, indicating that *Shep Ia* did not permeabilize *C. albicans* cell membranes (Fig. 2).

Fluo-Shep Ia cell internalization

When tested against *C. albicans* MDM8, *C. albicans* ATCC 90028 and *C. parapsilosis* ATCC 22019, *Fluo-Shep Ia* was four and twofold more active (MIC of 3.13 μM and 12.5 μM) and twofold less active (MIC of 12.5 μM) than *Shep Ia*, respectively. When exponential-phase *Candida* cells (2×10^6 CFU/mL) suspended in PDB were incubated with the fluorescently labeled analogue for 15 min at 37 °C, we observed a granular intracellular staining pattern, indicative of cellular internalization (Fig. 3), that was not observed when *Fluo* was used as control.

Blocking respiration using mitochondrial inhibitors for 1.5 h did not influence the viability of *C. albicans* (Helmerhorst et al. 1999a). When *Fluo-Shep Ia* was added at its MIC (3.13 μM) to the resulting suspension and incubation was continued for 15 min, the cells incubated at 0 °C or with NaN_3 showed 50 and 90 % lower peptide uptake (Fig. 4), respectively, indicating that the internalization process is temperature- and energy-dependent.

Peptide uptake by the fungal cells was not affected in 34.25 mM NaCl, so it seems that the hydrophobic nature of *Fluo* makes the fluorescently labeled analogue less sensitive to ionic strength changes.

Circular dichroism spectra of Shep Ia

The spectra of *Shep Ia* in 10 mM PBC buffer, pH 5.0, 60 % TFE, or 20 mM SDS in 10 mM PBC, pH 5.0, are shown in Fig. 5. Interestingly, although most peptides in aqueous solution display spectra with an intense minimum around 195 nm (Yang et al. 1986) that indicate an unordered conformation due to the fast equilibrium between various possible conformations, *Shep Ia* presented a low-intensity

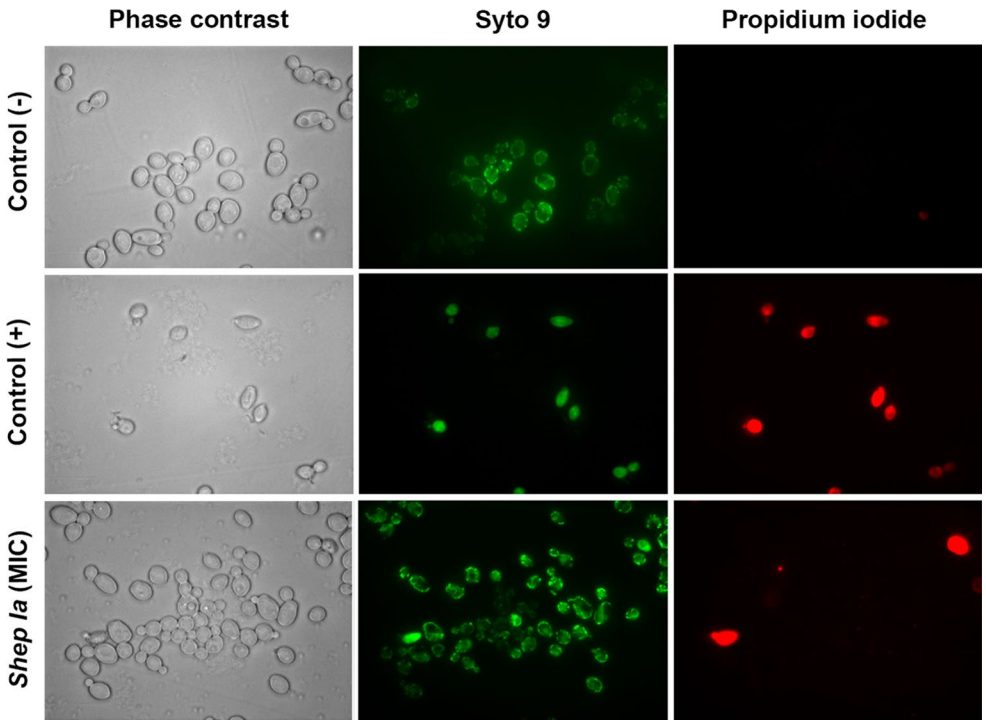

Fig. 2 Membrane permeability assay. Exponential phase *C. albicans* MDM8 cells (2×10^6 CFU/mL) suspended in PDB were incubated for 60 min at 37 °C with *Shep Ia* (12.5 μM, MIC value). Subsequently, the cells were treated with *SYTO® 9* e *propidium iodide* for 15 min. Water and isopropanol were used as negative and positive controls, respectively

spectrum showing two bands with positive maxima centered at ca. 198 and 225 nm and a minimum centered at ca. 212 nm. These features are suggestive of the presence of β-pleated sheets and β-turns.

Discussion

It is well-known that in plants, the three main families of proteins found in cell walls are glycine-rich proteins (GRPs; 60–70 % of glycine), extensins, and proline-rich proteins (Ringli et al. 2001). Many GRPs or their encoding genes and their respective subcellular localizations have already been described, so it is recognized that these proteins participate in central cellular processes. The fact that their expression is regulated by hormones, circadian rhythms, wounds, pathogen infection, and environmental stress (light, cold, salt, water) upholds their biological importance (Sachetto-Martins 2000; Ringli et al. 2001).

Despite the fact that *Shep I* is a glycine-rich AMP, there are no indications that this is part of the innate immune system of *Capsella bursa-pastoris*. In this study, analysis of the *Shep-GRP* amino acid sequence revealed that the *N*-terminal putative signal peptide is a conserved domain typical of the GRP superfamily (Finn et al. 2008). Such conservation points out that *Shep-GRP* could have the same localization and/or functions of GRPs, an hypothesis that is strengthened here by the results obtained with PSI-BLAST software, as they showed a high degree of identity between *Shep-GRP* and GRPs from *Arabidopsis thaliana* and *Arabidopsis lyrata lyrata* (Fig. 1). One example is the glycine-rich protein *AtGRP9* (NCBI reference sequence NP_001031332.1) from *A. thaliana*, a salt stress-responsive protein expressed in root vascular tissue that interacts with *AtCAD5*, a major cinnamyl alcohol dehydrogenase (CAD) involved in lignin biosynthesis (Chen et al. 2007). Since *C. bursa-pastoris* and *A. thaliana* belong to the family *Brassicaceae* (Slotte et al. 2006), *Shep I* could also have a similar biological function and be a promiscuous peptide, such as those found in plant defense, e.g., defensins (antimicrobial action, plant development control, and response to zinc stress) and cyclotides (antimicrobial, antihelmintic, insecticidal, and cytotoxic activities) (De Souza Cândido et al. 2011; Franco 2011). Promiscuous peptides are not only interesting for pharmaceutical purposes, but also for the development of agrochemicals, resistant transgenic plants, cosmetics, and other products (Franco 2011).

As previously reported (Remuzgo et al. 2009), stepwise solid-phase synthesis of glycine-rich peptides can be challenging because, depending on the protocols employed, the desired products are extensively contaminated with byproducts resulting from premature removal of the Fmoc-group

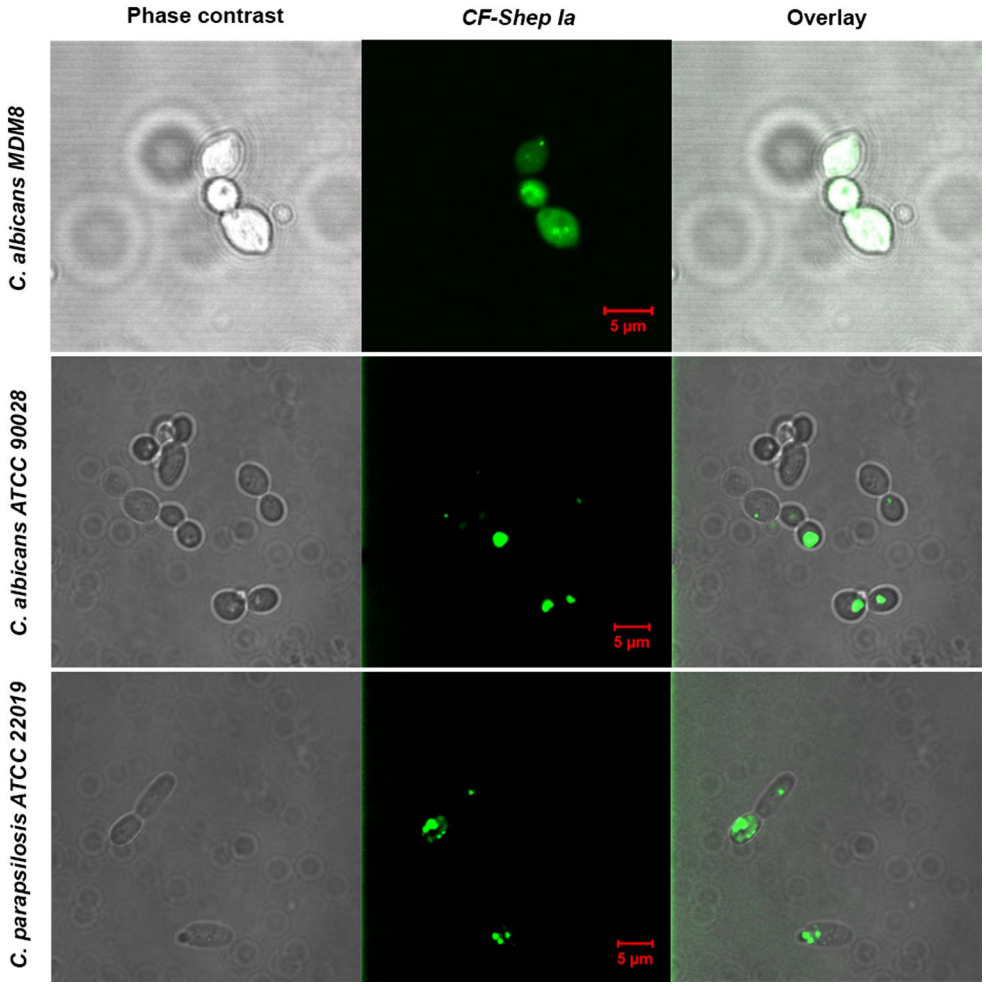

Fig. 3 Intracellular distribution of *Fluo-Shep Ia* as examined by confocal laser microscopy. Exponential phase *C. albicans* MDM8, *C. albicans* ATCC 90028 and *C. parapsilosis* ATCC 22019 cells (2×10^6 CFU/mL) suspended in PDB were incubated for 15 min with *Fluo-Shep Ia* (MIC value: 3.13 µM, 12.5 µM and 12.5 µM, respectively)

from Fmoc-Gly used for the incorporation of Gly in the growing peptide under basic conditions. The Elimination of such byproducts by liquid chromatography is not always an easy task; the present work demonstrates that our protocols minimize their occurrence.

Once obtained, purified, and properly identified, our synthetic *Shep I* and analogues were tested to examine the *Shep I* structure–activity relationship, a topic also not assessed previously. The Clinical and Laboratory Standard Institute (CLSI) recommends the use of dilution methods for the cell susceptibility test because they are more reproducible compared to diffusion methods in agar plates (CLSI 2008). Our liquid growth inhibition assays employed low-salt concentrations (as often do other authors when performing similar studies of cationic AMPs) to avoid competition with Na^+ ions for the interaction with the negatively charged groups of the cell wall and plasma membrane and, consequently, to allow observation of the effects of carboxyamidation and/or truncations on the potency and selectivity of *Shep I* (which would not be detected in high-ionic-strength conditions, such as those used in the CLSI or EUCAST microdilution methods). Melittin, Hb40-61a, and amphotericin B were used as controls.

When comparing our results with those found by Park et al. (2000), who first reported *Shep I*, we noted that ours agree with theirs, as our synthetic peptide and some analogues were active against *C. albicans* MDM8, *C. albicans* ATCC 90028, fluconazole-resistant *C. albicans* HU168, and other three *Candida* species involved in candidiasis (*C. parapsilosis* ATCC 22019, *C. krusei* ATCC 6258, and *C. tropicalis* Squibb 1600). However, none of the synthetic peptides acted on Gram-negative bacteria and mycelial fungi, which seems related to protocol differences (indeed, they used agar-plate assay, and MIC is strictly dependent on the method, pH, and microorganism strains used [Hoffman and Pfaller 2001]). Also

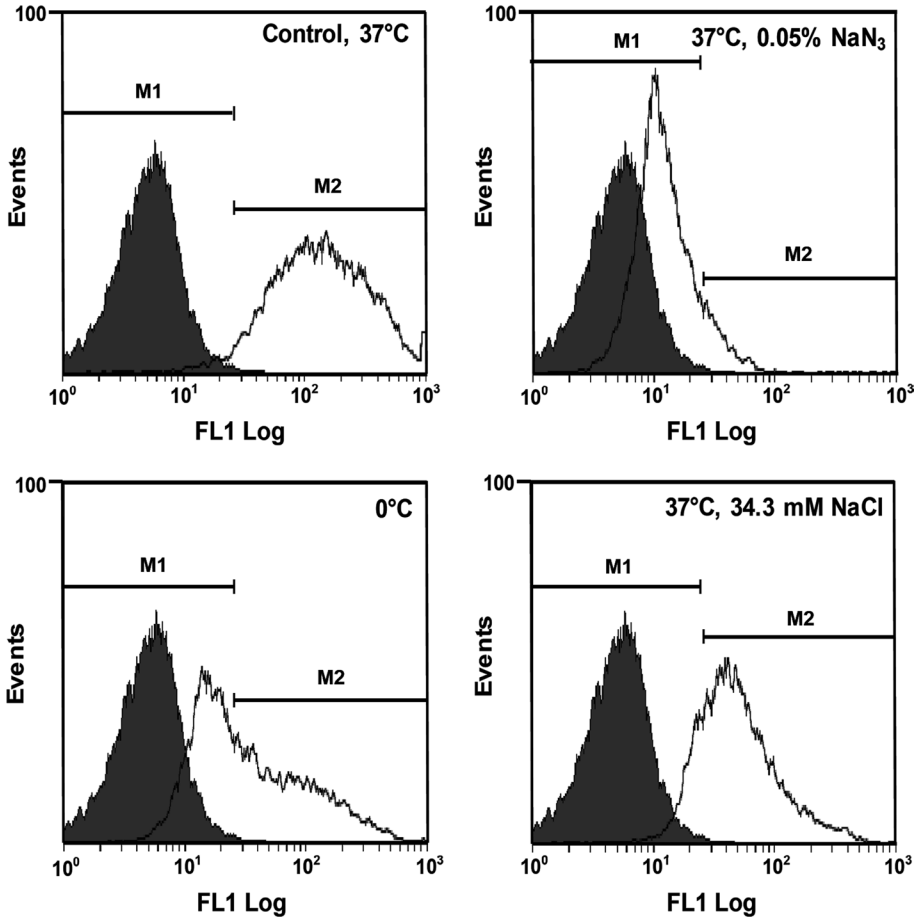

Fig. 4 Influence of low temperature (0 °C), ATP depletion, and presence of salt (34.25 mM) on cell uptake of *Fluo-Shep Ia* is shown. Exponential phase *C. albicans* MDM8 cells (2×10^6 CFU/mL) suspended in PDB were incubated with *Fluo-Shep I* (3.13 μM, MIC value) at 0 °C and 37 °C in the absence or presence of 0.05 % NaN_3 or 34.25 mM NaCl. The cells examined for the effect of low temperature and ATP depletion were pre-incubated for 30 min at 0 °C and in the presence of NaN_3, respectively

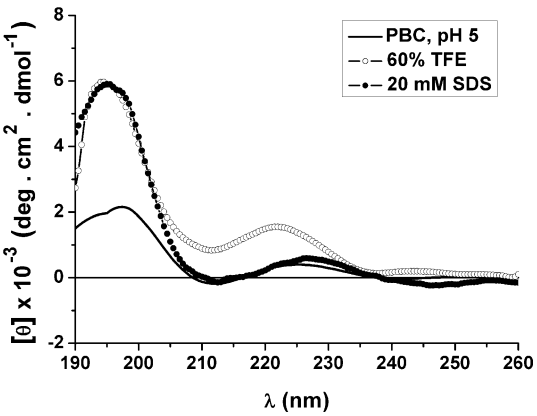

Fig. 5 CD spectra of *Shep Ia*. Spectra were recorded in three environments: 10 mM phosphate-borate-citrate buffer (PBC, solid line), pH 5.0, and 60 % trifluoroethanol (TFE, *open circle*), or 20 mM sodium dodecyl sulfate (SDS, *closed circle*) in 10 mM PBC, pH 5.0. Peptide concentration was 100 μM

in opposition to Park et al. (2000) observations, antifungal activity was affected by the simultaneous truncation of N- and C-terminal portions, indicating that: (1) the *N*-terminal dipeptide is of some importance to antifungal activity, and (2) the C-terminal end, Gly^{21}-Gly^{28}, is essential for the expression of antifungal activity. The difference in susceptibility of the *Candida* and *Saccharomyces* strains to *Shep I* and analogues found in this study may reflect a different interaction of these compounds with the cellular target (Hoffman and Pfaller 2001; Fitzgerald 2003).

The carboxyamidated analogue of *Shep I*, *Shep Ia,* was shown to be less salt-sensitive than *Shep I*, considerably more active if 10 μM $ZnCl_2$ was present, equipotent to *Shep I (3-28)a* against *Candida* strains, and twofold more active against *S. cerevisiae*, thus corroborating previous descriptions that carboxyamidation of AMPs may affect their properties due to overall positive charge increase and/or stabilization of active conformation (Kim et al. 2011; Machado et al. 2007). In fact, among many other examples are the following: (1) carboxyamidated PMAP-23, a cathelicidin family AMP, crosses external and internal cellular membranes of *Escherichia coli*, while free-carboxyl PMAP-23 only crosses the external cellular membrane (Kim et al. 2011); (2) amidated α-chain hemoglobin fragments 33–61 and 40–61 are fourfold more active against *Candida albicans* than the original ones (Machado et al. 2007). Thus, *Shep Ia* was mostly used in the next steps of the present investigation.

Our data also corroborate previous reports that the antimicrobial activity and/or ability of some AMPs to permeabilize or cross microbial cell membranes are affected by the presence of divalent cations, such as Mg^{2+} and Ca^{2+} (at physiological concentrations), and monovalent cations, such as Na^{+} and K^{+} (~100 mM). It must be mentioned that even though those reports raise the idea that only peptides that are able to directly kill microbes under physiological conditions where salt concentration is high should be called "antimicrobial peptides" and studied (Hancock and Sahl 2006), salt-sensitive AMPs have continued to be a topic of increasing interest because: (1) little is known about the conformation features that determine insensitivity to salt, and (2) applications exist with vehicles at low-ionic strength, e.g., topical administration, food preservatives, freshwater aquaculture, etc. (Kumar Sinha et al. 2009). As another example, the binding, internalization, and candidacidal activity of histatin-3, a histidine-rich peptide like *Shep I* and its analogues described here, are enhanced in low-ionic strength conditions (Oppenheim et al. 2012).

It was not surprising to find out that 10 μM $ZnCl_2$ potentiates the activity of *Shep I* and *Shep Ia* against *C. albicans* MDM8 and *C. albicans* HU168 (the last being a fluconazole-resistant strain), and also makes -*Shep Ia* and *Shep I (3-28)a* active against *C. albicans* ATCC 90028, because it is known that Zn^{2+} increases the antimicrobial activity of some His-rich peptides and proteins, and that peptide sequences with the conserved zinc binding motif of zinc-endopeptidases (HEXXHXXGXXH) coordinate this divalent metal ion with the histidines of their structures (Rydengard et al. 2006). Antifungal assays were also done in presence of Zn^{2+} ions. Besides, this divalent metal ion is an essential micronutrient, a component of more than 300 enzymes and an even greater number of proteins, is more abundant in the tissues compared to copper (8:1), and is considered relatively non-toxic to humans compared with other metals including copper (Plum et al. 2010). Therefore, the positive effect of Zn^{2+} ions on the antifungal activity of *Shep Ia* seems to be the result of peptide coordination with it and the consequent stabilization of structures needed for an effective interaction with the negatively charged compounds involved in antifungal activity triggering (Rydengard et al. 2006), a topic that is under investigation in our laboratories.

Since in high-ionic-strength buffer, such as phosphate-buffered saline, the true erythrocyte toxicity of salt-sensitive AMPs can be masked, *Shep I*, *Shep Ia*, *Shep I (3-28) a,* and *Shep I (6-28)a* were also tested in isotonic glucose buffer (Helmerhorst et al. 1999b) and confirmed to have low hemolytic activity. The fact that *Shep Ia* also displayed candidacidal activity highlights its therapeutic potential.

Usually, the mechanism of action of the cationic AMPs includes insertion into the membrane, triggering disruption of lipid bilayer physical integrity, membrane thinning/formation of transient pores that induce the permeabilization of cell membranes, or even the translocation of peptides across membranes/action on internal targets (Hancock and Sahl 2006). The results of the Live/Dead cell viability assay described here, in which cells with impermeable membranes are stained only with SYTO® 9 (green fluorescence) and cells with permeable membranes are stained with SYTO® 9 and propidium iodide (red fluorescence), indicate that *Shep Ia* does not permeabilize *C. albicans* cell membranes.

Aiming to verify *Shep Ia* distribution in the yeast cells, its fluorescently labeled analogue *Fluo-Shep Ia* was also successfully synthesized at 60 °C. Probably due to the structural changes caused by the insertion of the hydrophobic motif (Szeto et al. 2005), this analogue was more active than *Shep Ia*. Since the activity of *Shep Ia* against *C. albicans* was suppressed at NaCl concentrations ≥34.25 mM, the internalization of *Fluo-Shep Ia* in *C. albicans* cells suspended in PDB containing 4.28–34.25 mM NaCl was investigated and proved. The results demonstrating *Shep Ia* internalization in *C. albicans* cells took place in an energy- and temperature-dependent manner that suggested cellular metabolic processes similar to endocytosis. The granular staining pattern obtained pointed out that a specific organelle, possibly a vacuole, is its target (mitochondria were discarded using a Mitotracker orange CMTMRos, a cell-permeant mitochondrion-selective dye; data not shown).

Other histidine-rich antimicrobial peptides, such as tenecin-3, histatin-5, and the histidine-rich cell penetrating peptides (CPPs) LAH4 and H5WYG are internalized via endocytosis (Kim et al. 2001; Kumar et al. 2011; Bechinger 2013). In mammalian cells, this process takes place via peptide binding to the cell membrane through a non-specific electrostatic interaction, probably with heparin sulfate proteoglycans. After peptide internalization, the endosome is acidified and the peptide net charge is enhanced, causing destabilization of internal membranes and leading to disruption of the endosome and peptide release in the cytoplasm (Bechinger 2013). Like mammalian cells, yeasts have a receptor-mediated endocytosis pathway; their cell walls have other polysaccharides such as mannan, laminarin (β-1,3-glucan), sialic acid, and pustulan (β-1,6-glucan) (Jang et al. 2010). Since the binding of histatin-5 to *C. albicans* is mediated by laminarin, and its internalization occurs by both translocation and endocytosis (Jang et al. 2010), the mechanisms of action of *Shep I* and *Shep Ia* may be similar.

To date, practically nothing is known about the secondary structure of GRPs. A few reports indicate that glycine-rich domains have β-pleated sheet structures, but this is based on models obtained from secondary structure prediction programs and hydropathy profiles (Sachetto-Martins

2000; Ringli et al. 2001). As is expected for highly repetitive sequences that hinder the assignment of spectral frequencies, all attempts to investigate the *Shep Ia* structure by NMR failed (data not shown). Conversely, the CD spectra observed for *Shep Ia* are similar to those of cyclic AMPs containing disulfide bridges such as tachyplesin (Rao 1999), as well as the CD spectra of muscarinic toxin 7, which has a three-finger fold structure comprising five β-strands forming a twisted β-sheet (Fruchart-Gaillard et al. 2012). Nevertheless, data in the literature indicate that Gly residues are frequently present in β-turns, usually at position 3 (Falcomer et al. 1992). Thus, although *Shep Ia* is a linear peptide, the high glycine content probably exerts a strong influence on the peptide conformation, leading to the formation of β-turns even in aqueous solution. This is in agreement with conformation predictions making use of programs (Geourjon and Deleage 1995) that point to the propensity of turn formation in *Shep Ia*, especially in the C-terminal portion of the peptide. In the presence of TFE or SDS, the positive maximum became much more intense and was shifted to a lower wavelength (ca. 195 nm), suggesting stabilization of the β-pleated sheet(s). However, while the second, less intense maximum was slightly shifted to ca. 226 nm in the presence of SDS micelles, in 60 % TFE this band was centered at ca. 222, suggesting that (slightly) different conformations were stabilized in both media.

In summary, *Shep Ia* is highly active against *S. cerevisiae* and *Candida* strains (including fluconazole-resistant *C. albicans*). Its effectiveness is reduced at high ionic strength, but potentiated by Zn^{2+} ions. *Shep Ia* also kills those cells without displaying high hemolytic activity; the truncated analogue *Shep I (6-28)a* seems to be its minimally active portion. Our preliminary results suggest that the mechanism of action of *Shep Ia* in *C. albicans* includes cell internalization in a temperature- and metabolic energy-dependent process, as well as interaction with an intracellular target. Therefore, we believe that our study is a step forward in the search for a better understanding of the chemistry and biology of glycine- and histidine-rich AMPs. Furthermore, it contributes to the field of solid-phase peptide synthesis at high temperature.

Acknowledgments This work was supported by FAPESP (grants 04/14376-7 and 08/11695-1 to MTM) and CNPq (142022/2003-9, a doctoral fellowship for CR). We thank Dr. Nilton Lincopan (for providing *C. albicans* ATCC 90028 and HU 168 strains), Dr. Cleber W. Liria (for amino acid analyses), Adriana Y. Matzukuma and Roberto C. Modia (for assistance with FACS and confocal microscopy, respectively), and Gustavo P.B. Carretero (for theoretical structure prediction).

Conflict of interest The authors declare that they have no conflicts of interest.

References

Altschul SF, Madden TL, Schäffer AA, Zhang J, Zhang Z, Miller W, Lipman DJ (1997) Gapped BLAST and PSI-BLAST: a new generation of protein database search programs. Nucleic Acids Res 25:3389–3402

Baumann T, Kämpfer U, Schürch S, Schaller J, Largiadèr C, Nentwig W, Kuhn-Nentwig L (2010) Ctenidins: antimicrobial glycine-rich peptides from the hemocytes of the spider *Cupiennius salei*. Cell Mol Life Sci 67:2787–2798

Bechinger B (2013) Nanosized vectors for transfection assembled from peptides and nucleic acids. In: Aleman C, Bianco A, Venanzi M (eds) Peptide materials: from nanostructures to applications. J Wiley, West Sussex, pp 247–264

Bulet P, Hetru C, Dimarcq JL, Hoffmann D (1999) Antimicrobial peptides in insects; structure and function. Dev Comp Immunol 23:329–344

Chen AP, Zhong NQ, Qu ZL, Wang F, Liu N, Xia GX (2007) Root and vascular tissue-specific expression of glycine-rich protein AtGRP9 and its interaction with AtCAD5, a cinnamyl alcohol dehydrogenase, in *Arabidopsis thaliana*. J Plant Res 120:337–343

Clinical and Laboratory Standards Institute (2008) Reference method for broth dilution antifungal susceptibility testing of yeasts; Approved standard—3rd edition. CLSI *document M27-A3*. CLSI, Wayne

Colombo AL, Janini M, Salomao R, Medeiros EAS, Wey SB, Pignatari ACC (2009) Surveillance programs for detection and characterization of emergent pathogens and antimicrobial resistance. Results from the division of infectious diseases. UNIFESP An Acad Bras Cienc 81:571–587

De Souza Cândido E, Pinto MFS, Pelegrini PB, Lima TB, Silva ON, Pogue R, Grossi-de-Sá MF, Franco OL (2011) Plant storage proteins with antimicrobial activity: novel insights into plant defense mechanisms. FASEB J 25:3290–3305

Edgar RC (2004) MUSCLE: multiple sequence alignment with high accuracy and high throughput. Nucleic Acids Res 32:1792–1797

Ehret-Sabatier L, Loew D, Goyffon M, Fehlbaum P, Hoffmann JA, van Dorsselaer A, Bulet P (1996) Characterization of novel cysteine-rich antimicrobial peptides from scorpion blood. J Biol Chem 271:29537–29544

Eschenauer GA, Nguyen MH, Shoham S, Vazquez JA, Morris AJ, Pasculle WA, Kubin CJ, Klinker KP, Carver PL, Hanson KE, Chen S, Lam SW, Potoski BA, Clarke LG, Shields RK, Clancy CJ (2014) Real-World experience with echinocandin MICs against *Candida* species in a multicenter study of hospitals that routinely perform susceptibility testing of bloodstream isolates. Antimicrob Agents Chemother 58:1897–1906

Falcomer CM, Meinwald YC, Choudhary I, Talluri S, Milburn PJ, Clardy J, Scheraga HA (1992) Chain reversals in model peptides: studies of cystine-containing cyclic peptides. 3. Conformational free energies of cyclization of tetrapeptides of sequence Ac-Cys-Pro-X-Cys-NHMe. J Am Chem Soc 114:4036–4042

Fehlbaum P, Bulet P, Michaut L, Lagueux M, Broekaert WF, Hetru C, Hoffmann JA (1994) Insect immunity. Septic injury of Drosophila induces the synthesis of a potent antifungal peptide with sequence homology to plant antifungal peptides. J Biol Chem 269:33159–33163

Finn RD, Tate J, Mistry J, Coggill PC, Sammut SJ, Hotz HR, Ceric G, Forslund K, Eddy SR, Sonnhammer ELL, Bateman A (2008) The Pfam protein families database. Nucleic Acids Res 36:D281–D288

Fitzgerald DH, Coleman DC, O'Connell BC (2003) Susceptibility of *Candida dubliniensis* to salivary histatin 3. Antimicrob Agents Chemother 47:70–76

Franco OL (2011) Peptide promiscuity: an evolutionary concept for plant defense. FEBS Lett 585:995–1000

Fruchart-Gaillard C, Mourier G, Blanchet G, Vera L, Gilles N, Ménez R, Marcon E, Stura EA, Servent D (2012) Engineering of three-finger fold toxins creates ligands with original pharmacological profiles for muscarinic and adrenergic receptors. PLoS ONE 7:e39166

Geourjon C, Deleage G (1995) SOPMA: significant improvements in protein secondary structure prediction by consensus prediction from multiple alignments. Comput Appl Biosci 11:681–684

Hancock REW, Sahl HG (2006) Antimicrobial and host-defense peptides as new anti-infective therapeutic strategies. Nat Biotech 24:1551–1557

Helmerhorst EJ, Reijnders IM, van 't Hof W, Veerman ECI, Nieuw Amerongen AV (1999a) A critical comparison of the hemolytic and fungicidal activities of cationic antimicrobial peptides. FEBS Lett 449:105–110

Helmerhorst EJ, Breeuwer P, van't Hof W, Walgreen-Weterings E, Oomen LC, Veerman EC, Amerongen AV, Abee T (1999b) The cellular target of histatin 5 on *Candida albicans* is the energized mitochondrion. J Biol Chem 27:7286–7291

Herbinière J, Braquart-Varnier C, Grève P, Strub J-M, Frère J, Van Dorsselaer A, Martin G (2005) Armadillidin: a novel glycine-rich antibacterial peptide directed against gram-positive bacteria in the woodlouse *Armadillidium vulgare* (Terrestrial Isopod, Crustacean). Dev Comp Immunol 29:489–499

Hoffman HL, Pfaller MA (2001) In vitro antifungal susceptibility testing. Pharmacotherapy 21:111S–123S

Hoffmann-Santos H, Paula C, Yamamoto A, Tadano T, Hahn R (2013) Six-year trend analysis of nosocomial Candidemia and risk factors in two intensive care hospitals in Mato Grosso, Midwest region of Brazil. Mycopathologia 176:409–415

Iijima R, Kurata S, Natori S (1993) Purification, characterization, and cDNA cloning of an antifungal protein from the hemolymph of *Sarcophaga peregrina* (flesh fly) larvae. J Biol Chem 268:12055–12061

Jang WS, Bajwa JS, Sun JN, Edgerton M (2010) Salivary histatin 5 internalization by translocation, but not endocytosis, is required for fungicidal activity in *Candida albicans*. Mol Microbiol 77:354–370

Kim DH, Lee DG, Kim KL, Lee Y (2001) Internalization of tenecin 3 by a fungal cellular process is essential for its fungicidal effect on *Candida albicans*. Eur J Biochem 268:4449–4458

Kim JY, Park SC, Yoon MY, Hahm KS, Park Y (2011) C-terminal amidation of PMAP-23: translocation to the inner membrane of Gram-negative bacteria. Amino Acids 40:183–195

Kumar Sinha A, Norouzitallab P, Baruah K (2009) Antimicrobial peptides: possible therapeutics in aquaculture. World Aquacult 40:50–53

Kumar R, Chadha S, Saraswat D, Bajwa JS, Li RA, Conti HR, Edgerton M (2011) Histatin 5 uptake by *Candida albicans* utilizes polyamine transporters Dur3 and Dur31 proteins. J Biol Chem 286:43748–43758

Lee S, Moon H, Kurata S, Natori S, Lee B (1995) Purification and cDNA cloning of an antifungal protein from the hemolymph of *Holotrichia diomphalia* larvae. Biol Pharm Bull 18:1049–1052

Loffredo C, Assunção NA, Gerhardt J, Miranda MTM (2009) Microwave-assisted solid-phase peptide synthesis at 60 °C: alternative conditions with low enantiomerization. J Pept Sci 15:808–817

Lorenzini DM, Da Silva PI, Fogaca AC, Bulet P, Daffre S (2003) Acanthoscurrin: a novel glycine-rich antimicrobial peptide constitutively expressed in the hemocytes of the spider *Acanthoscurria gomesiana*. Dev Comp Immunol 27:781–791

Machado A, Sforça ML, Miranda M, Daffre S, Pertinhez TA, Spisni A, MTM M (2007) Truncation of amidated fragment 33-61 of bovine α-hemoglobin: effects on the structure and anticandidal activity. Biopolymers 88:413–426

Matejuk A, Leng Q, Begum MD, Woodle MC, Scaria P, Chou ST, Mixson AJ (2010) Peptide-based antifungal therapies against emerging infections. Drug Future 35:197–217

Nakagawa O, Ming X, Carver K, Juliano R (2013) Conjugation with receptor-targeted histidine-rich peptides enhances the pharmacological effectiveness of antisense oligonucleotides. Bioconjug Chem 25:165–170

Oppenheim FG, Helmerhorst EJ, Lendenmann U, Offner GD (2012) Anti-Candidal activity of genetically engineered histatin variants with multiple functional domains. PLoS ONE 7:e51479

Park CJ, Park CB, Hong SS, Lee HS, Lee SY, Kim SC (2000) Characterization and cDNA cloning of two glycine- and histidine-rich antimicrobial peptides from the roots of shepherd's purse, *Capsella bursa-pastoris*. Plant Mol Biol 44:187–197

Pelegrini PB, Murad AM, Silva LP, Dos Santos RCP, Costa FT, Tagliari PD, Bloch C Jr, Noronha EF, Miller RNG, Franco OL (2008) Identification of a novel storage glycine-rich peptide from guava (*Psidium guajava*) seeds with activity against Gram-negative bacteria. Peptides 29:1271–1279

Plum LM, Rink L, Haase H (2010) The essential toxin: impact of zinc on human health. Int J Environ Res Public Health 7:1342–1365

Rao AG (1999) Conformation and antimicrobial activity of linear derivatives of tachyplesin lacking disulfide bonds. Arch Biochem Biophys 361:127–134

Remuzgo C, Andrade GFS, Temperini MLA, Miranda MTM (2009) Acanthoscurrin fragment 101–132: total synthesis at 60 °C of a novel difficult sequence. Biopolymers 92:65–75

Ringli C, Keller B, Ryser U (2001) Glycine-rich proteins as structural components of plant cell walls. Cell Mol Life Sci 58:1430–1441

Rydengard VN, Andersson Nordahl E, Schmidtchen A (2006) Zinc potentiates the antibacterial effects of histidine-rich peptides against Enterococcus faecalis. FEBS J 273(11):2399–2406

Sachetto-Martins GF, Franco LO, De Oliveira DE (2000) Plant glycine-rich proteins: a family or just proteins with a common motif? Biochim Biophys Acta 1492:1–14

Slotte T, Ceplitis A, Neuffer B, Hurka H, Lascoux M (2006) Intrageneric phylogeny of *Capsella* (Brassicaceae) and the origin of the tetraploid *C. bursa-pastoris* based on chloroplast and nuclear DNA sequences. Am J Bot 93:1714–1724

Sousa JC, Berto RF, Gois EA, Fontenele-Cardi NC, Honório-Júnior JER, Konno K, Richardson M, Rocha MFG, Camargo AACM, Pimenta DC, Cardi BA, Carvalho KM (2009) Leptoglycin: a new Glycine/Leucine-rich antimicrobial peptide isolated from the skin secretion of the South American frog *Leptodactylus pentadactylus* (Leptodactylidae). Toxicon 54:23–32

Souza MP, Tavares MFM, Miranda MTM (2004) Racemization in stepwise solid-phase peptide synthesis at elevated temperatures. Tetrahedron 60:4671–4681

Sperstad SV, Haug T, Vasskog T, Stensvåg K (2009) Hyastatin, a glycine-rich multi-domain antimicrobial peptide isolated from the spider crab (*Hyas araneus*) hemocytes. Mol Immunol 46:2604–2612

Szeto HH, Schiller PW, Zhao K, Luo G (2005) Fluorescent dyes alter intracellular targeting and function of cell-penetrating tetrapeptides. FASEB J 19:118–120

Varanda LM, Miranda MT (1997) Solid-phase peptide synthesis at elevated temperatures: a search for and optimized synthesis condition of unsulfated cholecystokinin-12. J Pept Res 50:102–108

Yang JT, Wu CS, Martinez HM (1986) Calculation of protein conformation from circular dichroism. In: Hirs CHW, Timasheff SN (eds) Enzyme structure part k methods in enzymology. Academic Press, New York, pp 208–269